

PAPER • OPEN ACCESS

Feasibility study of an XPCI diagnostic to observe the evolution of micro-voids in an ICF target


To cite this article: F Barbato *et al* 2024 *Plasma Phys. Control. Fusion* **66** 025017

View the [article online](#) for updates and enhancements.

You may also like

- [A first investigation of accuracy, precision and sensitivity of phase-based x-ray dark-field imaging](#)
Alberto Astolfo, Marco Endrizzi, Gibril Kallon *et al.*
- [Locality estimates for Fresnel-wave-propagation and stability of x-ray phase contrast imaging with finite detectors](#)
Simon Maretzke
- [The effect of the spatial sampling rate on quantitative phase information extracted from planar and tomographic edge illumination x-ray phase contrast images](#)
C K Hagen, P C Diemoz, M Endrizzi *et al.*

Feasibility study of an XPCI diagnostic to observe the evolution of micro-voids in an ICF target

F Barbato^{1,*} , L Savino¹, A Schiavi¹ and S Atzeni^{1,2}

¹ Dipartimento SBAI, Università di Roma 'La Sapienza', Roma, Italy

² Focused Energy GmbH, Darmstadt, Germany

E-mail: francesco.barbato@uniroma1.it

Received 29 September 2023, revised 5 December 2023

Accepted for publication 3 January 2024

Published 18 January 2024



CrossMark

Abstract

Bulk perturbations (voids or crystalline structure) inside the ablator of a capsule used for inertial confinement fusion are seeds for instabilities that can hinder the ignition. The study of these defects and their evolution during the implosion is one of the steps needed to achieve fusion. The current methods used by the field are to infer these effects indirectly with measurements of implosion velocity and neutron yield, among others. Observing them directly with an x-ray imaging diagnostic is difficult due to the small scale length of these defects. In this work we study the feasibility of a new diagnostic based on x-ray phase-contrast imaging. This technique has been demonstrated to perform better than standard x-ray absorption techniques in critical situations like this. By using a synthetic diagnostic we show the capabilities of this new possible approach and the limits in relation to the parameters of currently available laser facilities.

Keywords: x-ray phase-contrast, synthetic diagnostics, ICF

1. Introduction

In inertial confinement fusion (ICF) bulk perturbations (voids or crystalline structure) inside the ablator of the capsule are seeds for instabilities [1–3]. In particular, for high-density Carbon and Beryllium ablators, bulk perturbations seem to dominate over surface perturbations [4]. Most of the diagnostics used to study these effects employ indirect measurements (VISAR, interferometry etc) which give only an ‘average’ effect of the instabilities [5]; imaging techniques (working in self emission or absorption contrast) provide a low resolution and limited sensitivity and contrast [4].

A possible solution could be the use of x-ray phase-contrast imaging (XPCI). In XPCI two phenomena contribute to the

contrast of the image, namely the relative difference in absorption of the features composing the target (as in standard absorption radiography), and the phase-shift that the same features induce on the transmitted x-ray waves. In absorption-based imaging the contrast vanishes as soon as the difference between the absorption coefficients of the features and the background approaches zero, or if the feature is thin. In XPCI the detected intensity is a function of the first or even the second derivative of the electron density (depending on the technique employed) [6]. The consequence is that XPCI is more sensitive to density gradients than absorption-based imaging [7].

A recent proof-of-principle experiment [8] demonstrated the feasibility of a multi-frame ultra-fast microscope based on XPCI. That work showed the time evolution of the interaction of a laser-driven shock-wave with a single micro-void encased in a planar target. The size of the micro-void ranged between 20 and 40 μm . The LCLS XFEL was used as a probe.

In this work, we want to test the capabilities of an XPCI diagnostic in a more realistic scenario, based on multiple defects on a spherically imploded shell. To design a working

* Author to whom any correspondence should be addressed.



Original Content from this work may be used under the terms of the [Creative Commons Attribution 4.0 licence](https://creativecommons.org/licenses/by/4.0/). Any further distribution of this work must maintain attribution to the author(s) and the title of the work, journal citation and DOI.

XPCI diagnostic it is necessary to minimize the absorption of the target and maximize phase-contrast. Multiple parameters affect these two phenomena, for this reason a synthetic diagnostic is fundamental to optimize all of them before proceeding with the experiment. We used the synthetic diagnostic PhaseX [9], that can reproduce images obtained from standard x-ray absorption imaging or phase-contrast imaging and was already benchmarked against experimental data [10–13]. Even though this work is fully numerical, it can help us to define a practical working range, useful for planning future experiments. In particular, we study the performance of the setup available today, and possible improvements.

2. Methods

The phase-shift induced by the object in the transmitted waves cannot be measured directly, so XPCI requires a specific setup to convert the phase-shift in a measurable variation of light intensity [6]. These setups are based either on specific analyzers (interferometers, crystal etc), or on the interference occurring between the waves after propagating a sufficient distance beyond the target.

The study presented here is based on the so-called propagation based imaging (PBI) [6]. If the distance between the target and the detector is large enough, the waves with different phases interfere with each other with the consequent of redistributing the light intensity on the detector plane. PBI compared to other XPCI techniques does not require optical elements (interferometer or crystal). The main consequences are, maximization of the photon flux and easy implementation. Moreover, the optical scheme is similar to the point-projection scheme, largely used in the field.

To maximize the phase-contrast the first step is to reduce the absorption of the target. This can be achieved easily by increasing the photon energy of the x-ray probe. Next steps depend on the XPCI technique chosen. In the case of PBI, the phase-contrast is proportional to the target-detector distance [6].

On top of that we have to consider the effect of the source size. The source size plays like a low-pass filter that results in a blurred image. Moreover, the contrast of an XPC-image is function of the source lateral coherence at the target plane [12] $L_{\perp} = \lambda R_{ST} / \sigma_s$, where R_{ST} is the source-target distance, λ and σ_s are the source wavelength and size respectively. The higher the coherence, the higher the contrast.

Regarding the detector, today the assortment spans from imaging plates that present the highest sensitivity and the worst resolution ($\sim 100 \mu\text{m}$), to x-ray CCD and film that can offer the best resolution ($< 10 \mu\text{m}$). Here we want to observe features that have scale length of microns and sub-microns. So a high magnification is mandatory to overcome the intrinsic detector resolution. Of course we can reduce the magnification, but this requires a detector with a resolution not available today. On the other side, the source size is an aspect on which we can work. For this reason we decide to study a configuration that relaxes the detector requirement. In particular, our study does not depend on the detector and its intrinsic resolution.

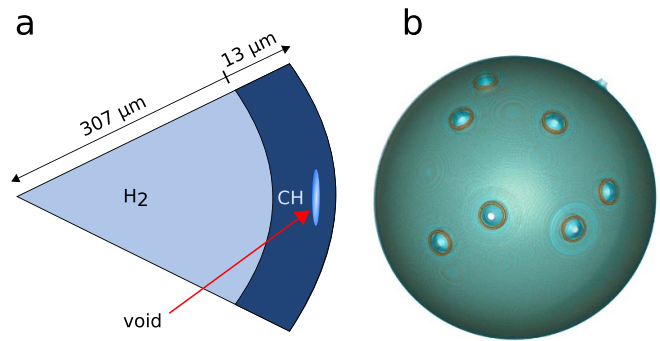


Figure 1. Target sketch: (a) 2D slice of the shell; (b) the void is replicated nine times over a 3D shell.

To summarize, we need to optimize four parameters: the photon energy, the source size, and the distances source-target and target-detector.

The work consist of two steps. In the first step, by using the hydrodynamic code DUED [14], we simulate the laser-driven spherical implosion of a plastic capsule that has a micro-void in the shell. In the second step, we use PhaseX to generate XPC-images from the output of the hydrodynamic simulations.

The density maps are generated from two-dimensional (2D) simulations of a single void. We based the simulations (target and laser) on an experiment performed at OMEGA [15]. The target (figure 1(a)) depicts the simulated target, a $13 \mu\text{m}$ thick CH plastic shell, with an outer radius of $320 \mu\text{m}$, filled with hydrogen gas. A single void is placed inside the shell, it lies on the symmetry axis of the 2D cylindrical code mesh. The shape of the void is Gaussian, the density at the center is 0.5 g cm^{-3} , 50% of that of the surrounding unperturbed shell. We simulate two types of voids with different size (see table 1) which we call *large* and *small* void respectively.

By using a Gaussian shape of the void, the hydrodynamic simulation is more stable, because this configuration avoids the collapse of the Lagrangian mesh when the shock-front interacts with the void.

We employ the synthetic diagnostic for a single time step on a 3D implosion by remapping a single time step over one fourth of a 3D sphere (figure 1(b)). In particular, the unperturbed region of the 2D simulation is used to generate the unperturbed region of the sphere. The cone containing the perturbation is displaced along nine random directions. In this way we create zones with different contrast. The perturbation that lies on the plane parallel to the detector plane faces the maximum contrast.

We use this hybrid 2D–3D approach for a practical reason. In general a fully 3D hydrodynamic simulation is hard to set-up especially if we want to reproduce the effects of volume defects in a shell. To achieve a proper resolution, it requires enormous computationally resources that are out of the scope of this work.

Moreover, the choice to use 2D hydrodynamic simulation to study target defects is not new in literature [8, 16]. A 2D simulation of course fails to reproduce correctly effects

Table 1. Voids specification: *FWHM*'s are the full width at half maximum along the shell radius R and the its orthogonal direction Z ; the parameter *density* indicates the density value at the center of the void.

void	FWHM-R (μm)	FWHM-Z (μm)	density (g cm^{-3})
small	1.25	0.25	0.5
large	5.00	1.00	0.5

that are intrinsically 3D and cannot reproduce an inter-voids interaction, however, in this work we are not interested in the effects that these defects have on the achievement of the ignition. We need a simple mock target that can reproduce realistically all drawbacks that an XPCI diagnostic platform may face.

As imaging setup we use the same configuration employed in a previous experiment at OMEGA [13]. The source-target distance is 2.2 cm, the target-detector distance is 259.6 cm, the source size is $10 \mu\text{m}$. We use as x-ray probe the titanium $K\alpha$ (4.5 keV) line to have a contrast of the image that benefits from absorption and phase contrast. As an example, by using the Copper $K\alpha$ (8.4 keV), another candidate widely used, we would reduce the absorption contrast drastically. In this case, to compensate the reduction of absorption contrast on the final images, we have to improve the phase contrast by stressing the requirements on the imaging setup parameters (source size and distances).

Regarding the time smearing, we did not see changes in the features of interest on a time scale of 50 ps, so the use of a back-lighter with a pulse duration of 10 ps (obtainable at OMEGA [17]) is safe.

3. Results

Figure 2 shows images generated using the *large* void. The images show the evolution of defects at four time steps, before the shock reaches the center of the sphere. For all images we assume an ideal point source (here the name *Ideal XPCI* and *Ideal absorption*). We begin by examining the case of an idealized point source, before investigating more realistic cases. We do this initially to put the two approaches on a comparable level. As we mentioned before, the phase-contrast is a function of the source size.

Figure 2 clearly shows the advantage of using XPCI instead of standard absorption imaging. If we observe the *Ideal absorption* images we do not see evidence of the perturbation at all. XPCI can instead detect and track the evolution of the defects and their position relative to the shock-front; phase-shifts from the density gradients in the voids increase the contrast of the defects above 80%. After 1.5 ns (figure 2 *Ideal XPCI*) we see the voids evolving in plasma jets outwards from the shell.

Regarding the behavior of the contrast with the defect orientation, we do not see difference up to 1.25 ns. At 2.0 ns the defects are so close that we cannot distinguish their orientation. We can see differences on the jet lengths that, in this

particular case, is given by the different orientations of each perturbations.

This first test shows us that XPCI has the capability to detect micro-void perturbations. Now we move to a more realistic scenario, by adding the effect of a source with a finite size. We choose a source size of $10 \mu\text{m}$, a value comparable to what was obtained in a previous experimental campaign [13]. To emphasize the capabilities of the the diagnostic, we move from the *large* to the *small* micro-void, the size of voids being now one fourth of the previous case. Figure 3 shows the density maps at different time steps of the 2D simulation of a single *small* micro-void. The micro-void evolves in a bubbles of low density material that precedes the shock front, and after 1.25 ns the bubble collapses in a jet of plasma outwards from the shell.

Figure 4(a) shows the result of this new test case. In this case we still see the shock-front, but the diagnostic cannot detect the perturbations at 1.0 and 1.25 ns. At 1.5 ns we see some faint spots (contrast $\sim 3\%$), but here the main contribution to the contrast comes from the absorption. At 2.0 ns we see a non uniform red line surrounding the sphere, a signature of the presence of perturbations, but nothing more.

So XPCI has the potential to detect the effect induced by micro-voids in a spherical implosion, but in a configuration available today (source and set-up) XPCI would not give significant results. The question is if there is any possibility to get some results by optimizing the set-up. As we mentioned briefly before, two parameters impact the contrast in an XPCI-image: the source size and the distances. Regarding the distances, the contrast increases as the target-detector distance increases. However, the deleterious effect of the source size also increases with the target-detector distance [12]. To compensate for this source effect we need to increase the source-target as well as the distance [12]. We decided to proceed this way, by keeping the same magnification we double the source-target distance (4.4 cm) and halve the source size ($5 \mu\text{m}$).

Figure 4(b) is the same image at 2.0 ns shown in figure 4(a), it is our reference point, the other images (figures 4(c)–(e)) come from the same target but with different imaging set-ups. In figure 4(c) we halve the source size, this increases the resolution and the contrast ($\sim 10\%$) at the edges, and we start to see the jets of plasma. In figure 4(d) we double the source-target distance, and consequently the target-detector distance to keep the same magnification, but the source size is again $10 \mu\text{m}$. In this case the contrast, $\sim 30\%$ at the edges, is higher than the previous two images, but we lost resolution, so the perturbations now are not defined. In the last image, figure 4(e), we have $5 \mu\text{m}$ source and 4.4 cm as source-target distance, the resolution and the contrast ($\sim 70\%$) now are enough to resolve the perturbations.

This simple study shows us the path to obtain an efficient XPCI diagnostic platform applied to ICF. Translating these two requirements into an experimental environment is not easy, especially at facilities like OMEGA or NIF. Mechanical constrains (vacuum chamber, surrounding diagnostics, etc) limit the distance ranges available today. As an example, 2.2 cm is the maximum source-target distance available today

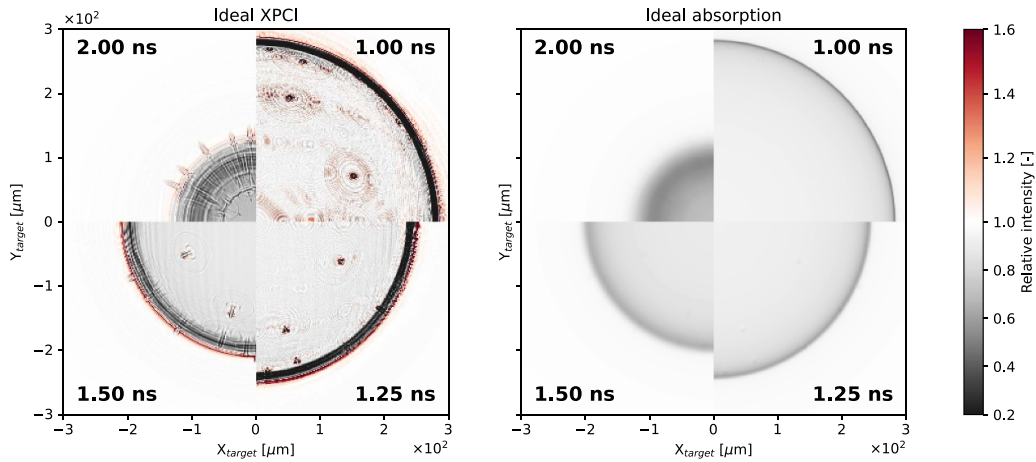


Figure 2. Comparison between ideal x-ray absorption image and XPC-image at different time steps. Both images are generated assuming an ideal x-ray point source, and the *large* void as the initial defect. The time step refers to the time after the laser pulse starts.

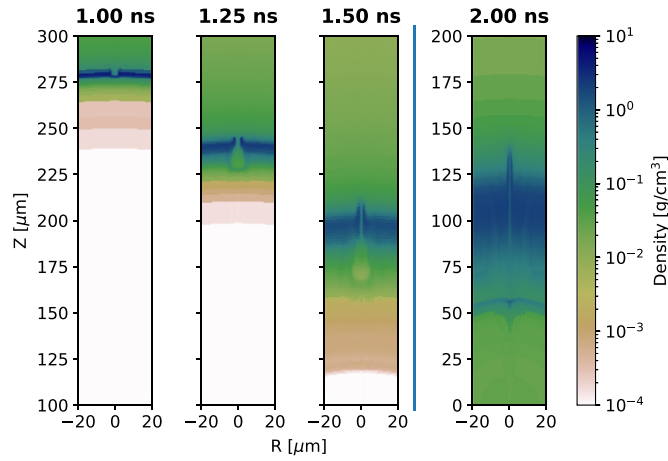


Figure 3. Density maps at different time steps of the the 2D simulation of a single *small* micro-void.

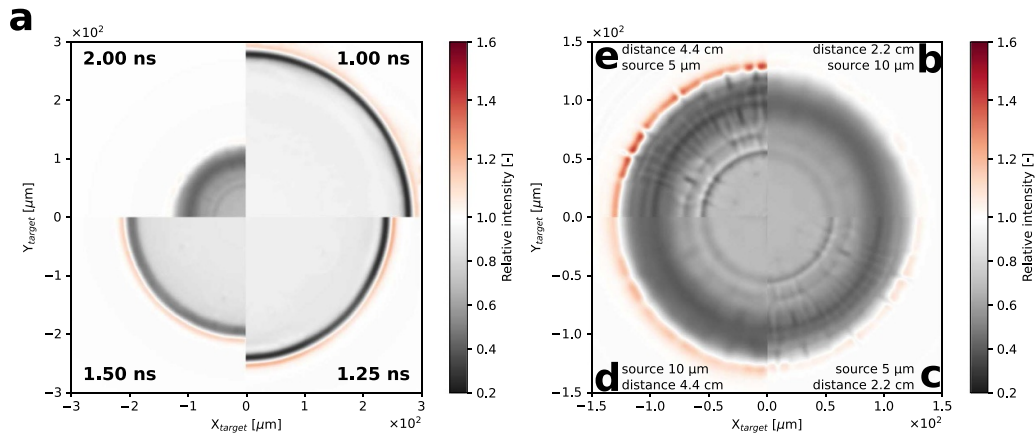


Figure 4. XPCI-images of the *small* void: (a) at different time step taking into account a finite source size (10 μm); (b) source size 10 μm and source-target distance 2.2 cm; (c) source size 5 μm and source-target distance 2.2 cm; (d) source size 10 μm and source-target distance 4.4 cm; (e) source size 5 μm and source-target distance 4.4 cm. The target-detector distance in figures (b)–(e) is adjusted to keep the magnification equal in all images.

at OMEGA. Regarding the source size, facilities like synchrotrons or XFELs can produce x-ray sources with sizes below 1 μm , the problem is that ICF facilities are not equipped with

these x-ray sources. An Achilles’ heel of laser-plasma x-ray sources is indeed the size of the source, especially when we use a high-intensity laser to generate hard x-rays [18].

An easy solution, that does not require the installation of an XFEL or a synchrotron, is to use a pinhole or a diffraction optic between the source and the target. The idea is to generate an ideal secondary source smaller than the original one. A pinhole is easy to implement, but has the drawback of limiting the photon flux. A converging diffraction optic (like Fresnel zone plate [19]) could be better, but its focal length is a function of the wavelength, the consequence being that a broadband probe can cause chromatic aberration.

Another solution is the use of a betatron x-ray source [20] but the current status suggests that this approach needs more work to be used as an XPCI source [21, 22].

To summarize, today we cannot achieve the performance of x-ray sources like XFEL or synchrotron, but we have room for improvement.

4. Conclusion

In this work we showed the capabilities of an XPCI diagnostics to track the evolution of micro-void defects in a spherically imploded shell. Our study demonstrated the advantages of XPCI over x-ray absorption imaging, the latter being completely blind to the defects. However, the scale length of these defects and the perturbations that they cause in the shell limits the capabilities of an XPCI diagnostic in a realistic scenario. At present time the ICF laser facilities provide x-ray sources with a size that is too big. We suggested some approaches to reduce the source size, some of them can be implemented easily, others require additional work and studies.

Data availability statement

All data that support the findings of this study are included within the article (and any supplementary files).

Acknowledgment

This work was partially supported by the European Union via the Euratom Research and Training Programme (Grant

Agreement No. 101052200–EUROfusion), within the framework of the Enabling Research Project: ENR-IFE.01.CEA ‘Advancing shock ignition for direct-drive inertial fusion’.

ORCID iD

F Barbato  <https://orcid.org/0000-0002-3005-2173>

References

- [1] Schiavi A and Atzeni S 2007 *Phys. Plasmas* **14** 070701
- [2] Igumenshchev I V, Goncharov V N, Shmayda W T, Harding D R, Sangster T C and Meyerhofer D D 2013 *Phys. Plasmas* **20** 082703
- [3] Haines B M, Sauppe J P, Albright B J, Daughton W S, Finnegan S M, Kline J L and Smidt J M 2022 *Phys. Plasmas* **29** 042704
- [4] Zylstra A B et al 2020 *Phys. Plasmas* **27** 092709
- [5] Smalyuk V A et al 2020 *High Energy Density Phys.* **36** 100820
- [6] Olivo A and Castelli E 2014 *Riv. del Nuovo Cim.* **37** 467–508
- [7] Montgomery D S 2023 *Rev. Sci. Instrum.* **94** 021103
- [8] Hodge D S et al 2022 *Opt. Express* **30** 38405
- [9] Barbato F, Atzeni S, Batani D and Antonelli L 2022 *Opt. Express* **30** 3388
- [10] Antonelli L et al 2019 *Europhys. Lett.* **125** 35002
- [11] Barbato F et al 2019 *J. Instrum.* **14** C03005–03005
- [12] Barbato F et al 2019 *Sci. Rep.* **9** 18805
- [13] Antonelli L et al 2020 in preparation
- [14] Atzeni S, Schiavi A, Califano F, Cattani F, Cornolti F, Del Sarto D, Liseykina T V, Macchi A and Pegoraro F 2005 *Comput. Phys. Commun.* **169** 153–9
- [15] Igumenshchev I et al 2023 *Phys. Rev. Lett.* **131** 015102
- [16] Haines B M, Aldrich C H, Campbell J M, Rauenzahn R M and Wingate C A 2017 *Phys. Plasmas* **24** 052701
- [17] Meyerhofer D D et al 2010 *J. Phys.: Conf. Ser.* **244** 032010
- [18] Park H et al 2006 *Phys. Plasmas* **13** 056309
- [19] Do A, Pickworth L A, Kozioziemski B J, Angulo A M, Hall G N, Nagel S R, Bradley D K, Mccarville T and Ayers J M 2020 *Appl. Opt.* **59** 10777
- [20] Rosmej O et al 2021 *Matter Radiat. Extremes* **6** 048401
- [21] Lemos N et al 2018 *Plasma Phys. Control. Fusion* **60** 054008
- [22] Albert F et al 2019 *Nucl. Fusion* **59** 032003